Article

Discovery Medicine 2024; 36(187): 1600–1609
https://doi.org/10.24976/Discov.Med.202436187.146

Remimazolam Alleviates Ventilator-Induced Lung Injury by Activating TSPO to Inhibit Macrophage Pyroptosis

Lei Zhang[1], Dong Zhao[1], Huayan Lv[1], Xiaofeng Jiang[1,*]

[1]Department of Anesthesiology, Affiliated Jinhua Hospital, Zhejiang University School of Medicine, 321000 Jinhua, Zhejiang, China
*Correspondence: jiangxiaofeng_jxff@163.com (Xiaofeng Jiang)
Published: 20 August 2024

Background: Macrophages are activated in ventilator-induced lung injury (VILI), accompanied by macrophage pyroptosis. Remimazolam (Re) plays a role in inhibiting macrophage activation. In this study, we aimed to investigate the mechanism of Re in VILI.

Methods: A VILI model (20 mL/kg mechanical ventilation) was created using C57BL/6 mice. Alveolar macrophages were isolated from bronchoalveolar lavage fluid (BALF) and received mechanical stretching to simulate the mechanical ventilation *in vitro*. VILI model mice were treated with Re (16 mg/kg) to assess the alveolar structure, wet/dry (W/D) weight ratio, endothelial barrier antigen (EBA) permeability index, BALF protein content, inflammatory factors, macrophage pyroptosis, pyroptosis-related factors, and translocator protein (TSPO) level using a series of biological experiments. Whether Re alleviated macrophage pyroptosis by regulating TSPO was determined by rescue experiments.

Results: Re alleviated VILI, as evidenced by improvement of abnormal morphology of lung tissues during VILI and decreases in the lung W/D weight ratio, lung EBA permeability index, and BALF protein content. Re attenuated pulmonary inflammation and macrophage pyroptosis during VILI via down-regulation of inflammatory factors (myeloperoxidase, malondialchehyche, 8-hydroxy-2 deoxyguanosine, interleukin-6, tumor necrosis factor-α, macrophage inflammatory protein-2, interleukin-1β, and interleukin-18), and pyroptosis factors (cleaved gasdermin D (GSDMD)/GSDMD value, NOD-like receptor thermal protein domain associated protein 3 (NLRP3), and caspase-1). Re activated TSPO in macrophages. TSPO overexpression rescued the cell stretch-inhibited macrophage viability and cell stretch-induced macrophage pyroptosis.

Conclusion: Re alleviates VILI by activating TSPO to inhibit macrophage pyroptosis.

Keywords: remimazolam; ventilator-induced lung injury; translocator protein; macrophages; pyroptosis

Introduction

In recent years, mechanical ventilation has been recognized as a promising strategy for the treatment of patients with acute lung injury. Yet, ventilator-induced lung injury (VILI), is a possible complication of mechanical ventilation in clinics [1,2]. Reportedly, there are a series of inflammatory responses that cause lung dysfunction during the development of VILI [3]. In addition, alveolar macrophages, instrumental in VILI, can be activated by mechanical ventilation [4] and may contribute to the pathogenesis of VILI [5,6]. Therefore, VILI could be treated using a specific drug that inhibits macrophage activation.

The previous study has reported that remimazolam (Re) can play an anti-inflammatory role through suppression of macrophage activation [7]. Re is a kind of ultra-short-acting anesthetic, which was approved in 2020 and is used for general anesthesia in adult patients [8]. At present, anesthesia and ventilation are commonly used during operations [9]. Re can attenuate bronchopneumonia by reducing pro-inflammatory factors [10]. However, there is still insufficient research on the mechanism of Re in VILI; this topic is further explored in this study.

During VILI, alveolar macrophages release certain pro-inflammatory factors, and this is accompanied by macrophage pyroptosis [11]. Pyroptosis, a newly described mode of programmed cell death, can exacerbate the inflammatory response and contribute to several inflammatory diseases [12,13]. The typical sign of pyroptosis is the activated NOD-like receptor thermal protein domain associated protein 3 (NLRP3) inflammasome [14]. Of note, a novel idea that the inhibition of pyroptosis can alleviate VILI has been put forward [12]. This suggests that Re can also repress pyroptosis by reducing the release of inflammatory factors [15]. Therefore, it is worthwhile to investigate whether Re can alleviate VILI by curbing macrophage pyroptosis.

Through analysis of the SwissTargetPrediction database (http://www.swisstargetprediction.ch/), we found that translocator protein (TSPO) is a target receptor of Re. TSPO, a kind of mitochondrial outer membrane protein, is considered to be a new pivotal regulator of pyroptosis [16,17]. A deficiency of TSPO can aggravate macrophage pyroptosis [17]. Accordingly, Re may play a role in

alleviating VILI by regulating TSPO to inhibit macrophage pyroptosis.

In this study, we focused on clarifying the influence of Re on the progression of VILI and explaining the underlying molecular mechanism. We performed a series of experiments to determine whether Re mitigates VILI by activating TSPO to inhibit macrophage pyroptosis.

Materials and Methods

Animals

Thirty C57BL/6 mice (male, 20–25 g, 8–12 weeks old, Hangzhou Medical College, Hangzhou, China) were fed in a room with a normal circadian environment. All mice could freely obtain standard food and water.

Animal Treatments and Grouping

After 1 week of feeding, the mice were randomized into five groups (sham, Re, low tidal volume (VL), VILI, and VILI + Re groups; n = 6/group), and underwent experiments based on a previous report with minor modifications [18]. Post 12-h fast, all mice were anesthetized (1.5% isoflurane), the neck skin was disinfected, and the trachea was exposed by cutting the skin along the midline. A small incision was made in the tracheal cartilage with scissors to slowly insert a sterilized venous catheter about 1 cm along the trachea. The catheter was tightly fixed with a surgical line and connected to a small animal ventilator (V-1000, Shanghai Yuyan Instruments, Shanghai, China).

In the sham group, mice were not given mechanical ventilation after tracheotomy and intubation. In the Re group, based on the same treatment conditions as the sham group, mice were additionally given an intraperitoneal injection with Re (16 mg/kg, SML3467, Sigma-Aldrich, St. Louis, MO, USA) [7]. In the VL group, mice received mechanical ventilation (7 mL/kg, 4 h) after tracheotomy and intubation, with a respiratory frequency of 140 times/min. In the VILI group, mice underwent mechanical ventilation (20 mL/kg, 4 h) after tracheotomy and intubation, with a respiratory frequency of 100 times/min [18]. In the VILI + Re group, based on a treatment similar to the VILI group, mice additionally received an intraperitoneal injection with Re (16 mg/kg).

According to the grouping, mice were treated with 4 h of mechanical ventilation. 12 h later, the anesthetized (intraperitoneal injection of pentobarbital sodium (50 mg/kg, P3761, Sigma-Aldrich)) mice were sacrificed using cervical dislocation to harvest lung tissues for pathological examination, the evaluation of endothelial barrier antigen (EBA) permeability index, and the measurement of inflammatory factors. The wet/dry (W/D) weight ratio was calculated based on right lung tissues. Bronchoalveolar lavage fluid (BALF) was collected for the assessment of protein concentration, measurement of inflammation factors, and macrophage isolation. The aggravated lung injury, increased lung tissue W/D weight ratio, and decreased EBA permeability provide indications regarding the success of model construction, and the representative results are shown in Fig. 1A–C, with a success rate of model construction of 83.3%.

Hematoxylin-Eosin (HE) Staining Assay

The pathological morphology of lung tissue was detected by an HE staining assay kit (C0105S, Beyotime, Shanghai, China). Harvested lung tissues were fixed using 4% paraformaldehyde (P0099, Beyotime, Shanghai, China). After embedding with paraffin and slicing, the lung tissue samples were dewaxed by xylene (A530011, Sangon Biotech, Shanghai, China), and immersed in 100/90/80/70% ethanol and distilled water. The washed samples underwent color development by HE staining solutions. The treated samples were further reacted with fresh xylene and sealed using neutral gum (E675007, Sangon Biotech, Shanghai, China) in sequence. Finally, the pathological morphology of lung tissue was photographed using a light microscope (Resolution: 100 µm, ×100; LV150, Nikon, Tokyo, Japan). The neutrophils in the alveolar space, neutrophils in the interstitial space, the existence of hyaline membranes, proteinaceous debris filling the airspaces, and alveolar septal thickening were observed for determination of a lung injury score [19]. Each variable was divided into levels of 0 (normal), 1 (mild injury), and 2 (severe injury) based on the severity of the injury. The sum of scores for the five independent variables is the lung injury score, with a possible total of 10 points. The lung injury score was calculated by two doctors at our hospital who were unaware of the group information.

Lung W/D Weight Ratio

The wet and dry (after 72-h baking in a 60 °C oven) weights of right lung tissue were obtained to calculate the W/D weight ratio.

Lung EBA Permeability Index

As described in a previous report, the EBA permeability index of the left lung was measured [18]. The lung tissues were homogenized (2 mL 1 × phosphate buffer saline (PBS), P1020, Solarbio, Beijing, China), treated (2 mL formamide, 18 h, 65 °C; A600212, Sangon Biotech, Shanghai, China), and centrifuged (15,000 ×g, 30 min, 4 °C) for collection of supernatant. Optical density at 620 nm (OD_{620}) was measured using a spectrophotometer (UV-1800, Macylab Instrument, Shanghai, China). The EBA permeability index = OD_{620} of EBA in lung tissues/OD_{620} of EBA in plasma [18].

Protein Concentration in BALF

Protein concentration detection in BALF was accomplished using a bicinchoninic acid (BCA) kit (C503021, Sangon Biotech, Shanghai, China). Briefly, the protein

sample was mixed with a BCA working solution (37 °C, 30 min). Finally, the OD_{562} was measured using a microplate reader (HTS-XT, Bruker Optics, Rheinstetten, Germany).

Enzyme-Linked Immunosorbent Assay (ELISA)

The inflammation-related factors included myeloperoxidase (MPO), malondialchehyche (MDA), 8-hydroxy-2 deoxyguanosine (8-OHdG), interleukin (IL)-6, tumor necrosis factor (TNF)-α, macrophage inflammatory protein (MIP)-2, IL-1β, and IL-18, which were measured by ELISA. After lung tissues were fully ground in 1 $\times$ PBS and centrifuged, the supernatant was subjected to quantification of MPO, MDA and 8-OHdG. TNF-α, MIP-2, IL-1β, and IL-18 in BALF were quantitated. Mouse MPO (YS02650B), MDA (YS02715B), 8-OHdG (YS02529B), IL-6 (YS02456B), TNF-α (YS05734B), MIP-2 (YS02592B), IL-1β (YS06169B), and IL-18 (YS02903B) ELISA kits were provided by YaJi Biological (Shanghai, China). Samples were incubated in the ELISA plate (30 min, 37 °C), and cultured in enzyme-labeled reagent (30 min, 37 °C), with each step followed by washing. Chromogenic agents A and B were sequentially added to the ELISA plate (darkness, 30 min, 37 °C). The termination solution was used to stop the reaction. Within 15 minutes, the OD_{450} was measured using a microplate reader.

Isolation and Culture of Mouse Alveolar Macrophages from BALF

As described in previous studies, the mouse alveolar macrophages were isolated from BALF [11,18]. Post BALF centrifugation (10 min, 200 $\times$g, 4 °C), the leukocytes were collected, where alveolar macrophages were isolated by negative magnetic bead sorting in the immunomagnetic separation system (BD Biosciences Pharmingen, San Jose, CA, USA). The purity of macrophages was identified to be more than 95% by flow cytometry (**Supplementary Fig. 1**), and these were used for further experiments. The isolated macrophages were incubated with RPMI-1640 medium (30-2001, ATCC, Manassas, VA, USA) containing 10% fetal bovine serum (30-202-0, ATCC) and 1% penicillin/streptomycin (PB180120, Procell, Wuhan, China) (37 °C, 5% CO_2), routinely subjected to mycoplasma contamination test and confirmed to be mycoplasma-free.

Macrophage Treatments and Grouping

Macrophage treatment involves two steps. In the first step, macrophages were transfected with/without pDONR223 vector/TSPO plasmid for 24 h. The coding sequence (CDS) region of the TSPO was inserted into the pDONR223 vector (#23829, Addgene, Watertown, MA, USA) to construct the overexpression plasmid. The pDONR223 vector was used for the negative control (NC). In the second step, macrophages were assigned to either control, cell stretch (CS), CS + NC, or CS + TSPO groups. Using the FX-5000T Flexercell Tension Plus system (Flexcell, Burlington, NC, USA), macrophages were stretched to simulate the mechanical ventilation *in vitro*. In brief, macrophages were loaded in the Flexercell FX-4000T strain unit and stretched (4 h) with a 20% range and frequency of 30 cycles/min (0.5 Hz). The stretch-to-relaxation ratio was 1:1 [20]. Control group: macrophages were loaded in the Flexercell FX-4000T strain unit without mechanical stretching. CS group: macrophages received mechanical stretching (4 h). CS + NC or TSPO group: macrophages received mechanical stretching (4 h) and were transfected with pDONR223 vector or TSPO plasmid (24 h).

Transfection

Macrophages plated (5×10^5 cells/well) in 6-well plates for 24 h received transfection as per grouping, employing X-tremeGENE 360 transfection reagent (XTG360-RO, Roche, Basel, Switzerland). Solution A was the mixture (5 min) of 5 µg pDONR223 vector/TSPO plasmid and 125 µL serum-free medium (SAFC Biosciences, 14530C, Boston, MA, USA). Solution B was the mixture (5 min) of 10 µL transfection reagent and 125 µL serum-free medium. The two solutions were fully mixed (15 min) and added to macrophages for 24-h transfection.

Flow Cytometry Assay

The collected macrophages (5×10^5) were suspended, and incubated (darkness) with the fluorescently labeled caspase-1 (FLICA®660, ICT-9122, ImmunoChemistry Technology, Hamburg, Germany) and propidium iodide (PI, A601112, Sangon Biotech, Shanghai, China). Next, a flow cytometry assay was conducted using a flow cytometer (PL00285, Thermo Fisher Scientific, Waltham, MA, USA). The caspase-1- and PI-positive cells represented macrophage pyroptosis.

Western Blot

Extraction and concentration detection of total protein in macrophages were conducted using RIPA Lysis Buffer (PC101, Epizyme, Shanghai, China) and a BCA kit, respectively. SDS-PAGE gel (RFT076, BioLab, Beijing, China)-separated total protein was transferred onto the nitrocellulose transfer membranes (SNM439, BioLab). Membranes were sequentially incubated with 5% skim milk (25 °C, 1 h), primary antibodies (overnight, 4 °C), and Goat anti rabbit secondary antibodies (25 °C, 1 h). Related antibodies are listed in Table 1. Gasdermin D (GSDMD) and cleaved GSDMD levels were normalized by heat shock protein 90 (HSP90) level. NLRP3, IL-1β, caspase-1, and TSPO levels were normalized by glyceraldehyde-3-phosphate dehydrogenase (GAPDH) level. After visualization by ECL reagent (YWB003, YFXBIO, Nanjing, China), the images were captured by a BeyoImage 600 Chemiluminescence imaging system (Beyotime) and dissected by ImageJ 1.8.0 software (National Institutes of Health, Bethesda, MD, USA). The

Table 1. Information regarding antibodies used in this study.

Name	Catalog	Molecular weight (kDa)	Dilution	Manufacturer
GSDMD	ab209845	53	1/1000	Abcam, Cambridge, UK
Cleaved GSDMD	ab209845	32	1/1000	Abcam, Cambridge, UK
HSP90	ab32568	92	1/100,000	Abcam, Cambridge, UK
NLRP3	ab263899	118	1/1000	Abcam, Cambridge, UK
IL-1β	ab315084	30	1/1000	Abcam, Cambridge, UK
Caspase-1	ab138483	51	1/1000	Abcam, Cambridge, UK
TSPO	MA5-24844	19	1/1000	Thermo Fisher Scientific, Waltham, MA, USA
GAPDH	ab9485	40	1/2500	Abcam, Cambridge, UK
Goat anti rabbit	ab97051	—	1/10,000	Abcam, Cambridge, UK

GSDMD, gasdermin D; HSP90, heat shock protein 90; NLRP3, NOD-like receptor thermal protein domain associated protein 3; IL, interleukin; TSPO, translocator protein; GAPDH, glyceraldehyde-3-phosphate dehydrogenase.

Table 2. The primer sequences of related genes.

Gene	Forward primer (5′-3′)	Reverse primer (5′-3′)
TSPO (mouse)	TTGGCCGATCTTCTGCTTGT	CAGCAGGCCCAATGGTCATA
GAPDH (mouse)	CCATGGGGAAGGTGAAGGTC	AGTGATGGCATGGACTGTGG

TSPO, translocator protein; *GAPDH*, glyceraldehyde-3-phosphate dehydrogenase.

normalized relative protein expression level was calculated using the formula: x' (normalized data) = (x (original data) – mean data (x))/std data (x, internal control).

Quantitative Real Time Polymerase Chain Reaction (qRT-PCR)

Total RNA from macrophages isolated using Trizol reagent (T9424, Sigma-Aldrich) underwent RNA concentration determination and mixing with one-step qRT-PCR reagents (Solarbio, T2210). The fluorescence was detected using the LightCycler480 (Roche). The data were analyzed by the $2^{-\Delta\Delta ct}$ method [21]. The primer sequences of TSPO and GAPDH are listed in Table 2. GAPDH was employed as the internal reference.

Cell Counting Kit-8 (CCK-8) Assay

Macrophage viability was assessed using a CCK-8 kit (E606335, Sangon Biotech, Shanghai, China). Macrophages (1×10^4 cells/well) in 96-well plates (12 h) were treated in light of grouping. 24 h later, macrophages were incubated with CCK-8 reagent (10 µL per sample, 2 h). OD_{450} was detected by a microplate reader.

Statistical Analysis

Data are presented as mean ± standard deviation and analyzed using GraphPad 8.0 (GraphPad Software, San Diego, CA, USA). All assays were repeated at least three times. Differences among groups were compared using one-way analysis of variance (ANOVA), and the Tukey test was used for pairwise comparisons. p-values < 0.05 were considered statistically significant.

Results

Re Alleviated VILI

HE staining results indicated that the alveolar structure was normal in the sham, Re, and VL groups (Fig. 1A,B). In contrast, the VILI groups displayed unordered alveolar structure, fused alveolar cavities, and many inflammatory cells (Fig. 1A,B, $p < 0.001$). Of note, the effects of VILI on lung tissue morphology were reduced by Re (Fig. 1A,B, $p < 0.001$). In contrast to the sham group, the lung W/D weight ratio (Fig. 1C, $p < 0.001$), lung EBA permeability index (Fig. 1D, $p < 0.001$), and BALF protein content (Fig. 1E, $p < 0.001$) were significantly elevated in the VILI group, and these effects were reversed by Re (Fig. 1C–E, $p < 0.001$). Moreover, compared with the Re group, the lung EBA permeability index and BALF protein content were significantly increased in the VILI + Re group (Fig. 1D,E, $p < 0.05$).

Re Mitigated Pulmonary Inflammation and Macrophage Pyroptosis during VILI

The inflammation-related factors were evaluated by ELISA. Our results revealed higher levels of MPO, MDA, and 8-OHdG in lung tissues (Fig. 1F–H, $p < 0.001$), and higher IL-6, TNF-α, MIP-2, IL-1β, and IL-18 levels in BALF (Fig. 1I–M, $p < 0.001$) in the VILI group. These inflammation-related factors were significantly lower in the Re group (Fig. 1F–M, $p < 0.001$). Also, Re attenuated the impact of VILI on inflammation-related factors based on the comparison between the VILI and VILI + Re groups (Fig. 1F–M, $p < 0.01$).

Moreover, macrophage pyroptosis was clearly triggered during VILI, as indicated by the significant

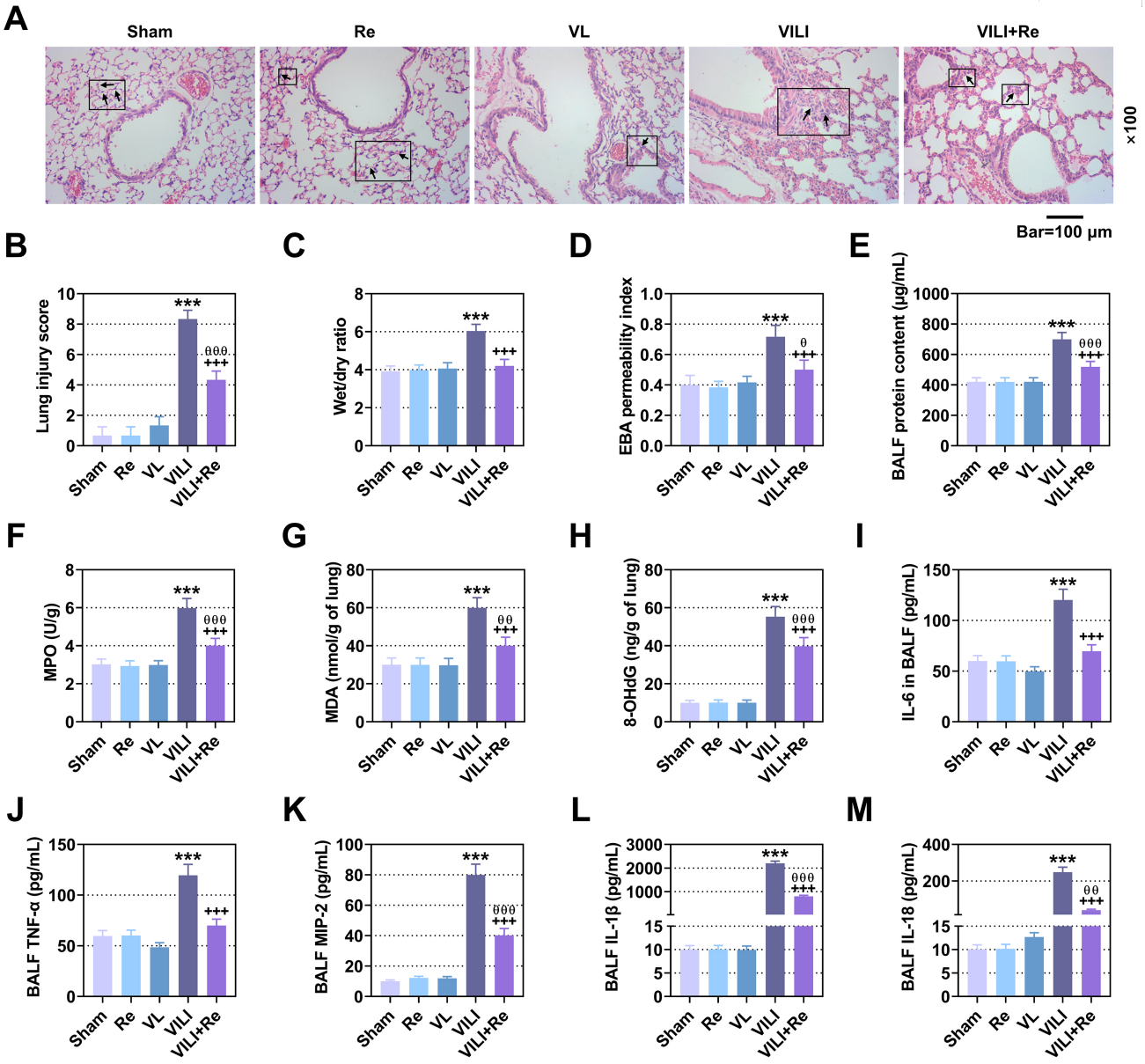

Fig. 1. Re alleviated VILI. For (A–L), C57BL/6 mice were classified into five groups (n = 6/group). Sham group: mice received no mechanical ventilation after tracheotomy and intubation. Re group: mice received no mechanical ventilation after tracheotomy and intubation, and were intraperitoneally injected with 16 mg/kg Re. VL group: mice underwent mechanical ventilation (7 mL/kg, 4 h) after tracheotomy and intubation, and the respiratory frequency was 140 times/min. VILI group: mice underwent mechanical ventilation (20 mL/kg, 4 h) after tracheotomy and intubation, and the respiratory frequency was 100 times/min. VILI + Re group: based on the VILI group, mice were intraperitoneally injected with 16 mg/kg Re. (A,B) The pathological morphology of lung tissue (HE staining assay). The arrows indicate the unordered alveolar structure, fused alveolar cavity, and inflammatory cells. Resolution: 100 μm, ×100. (C) The W/D weight ratio of right lung tissue. (D) Calculation of EBA permeability index of left lung based on the optical density (a spectrophotometer). (E) The protein content in BALF (BCA kit). (F–H) MPO (F), MDA (G) and 8-OHdG (H) levels in lung tissues (ELISA). (I–M) IL-6 (I), TNF-α (J), MIP-2 (K), IL-1β (L) and IL-18 (M) levels in BALF (ELISA). $^{***}p < 0.001$ vs. the Sham group. $^{+++}p < 0.001$ vs. the VILI group. $^{\theta}p < 0.05$, $^{\theta\theta}p < 0.01$, $^{\theta\theta\theta}p < 0.001$ vs. the Re group. All assays were repeated three times. Re, remimazolam; VL, low tidal volume; VILI, ventilator-induced lung injury; HE, hematoxylin-eosin; W/D, wet/dry; EBA, endothelial barrier antigen; BCA, bicinchoninic acid; BALF, bronchoalveolar lavage fluid; MPO, myeloperoxidase; MDA, malondialchehyche; 8-OHdG, 8-hydroxy-2 deoxyguanosine; IL, interleukin; TNF-α, tumor necrosis factor-α; MIP-2, macrophage inflammatory protein-2; ELISA, enzyme-linked immunosorbent assay.

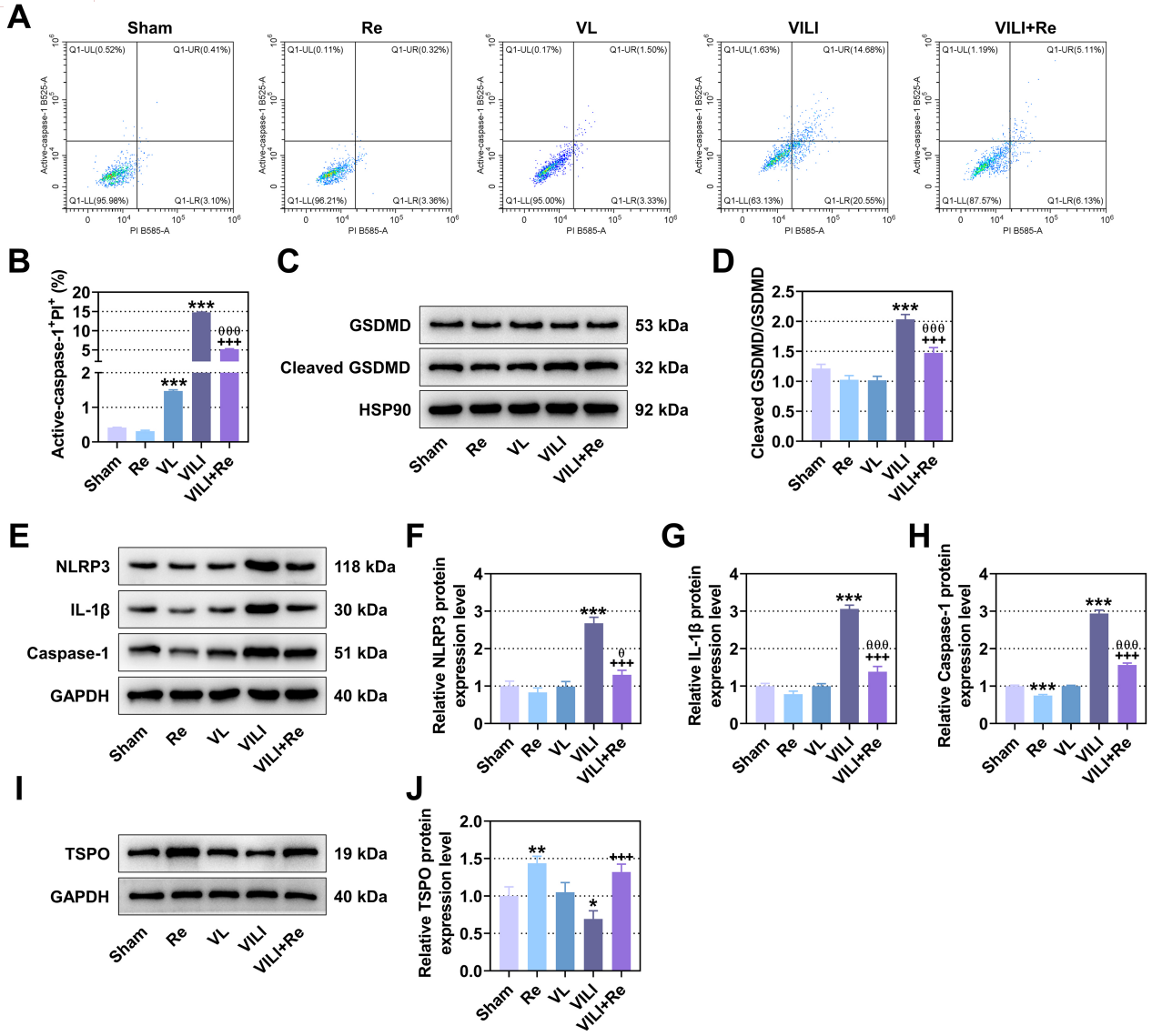

Fig. 2. Re repressed macrophage pyroptosis during VILI. For (A–J), C57BL/6 mice were classified into five groups (n = 6/group). Sham group: mice received no mechanical ventilation after tracheotomy and intubation. Re group: mice received no mechanical ventilation after tracheotomy and intubation, and were intraperitoneally injected with 16 mg/kg Re. VL group: mice underwent mechanical ventilation (7 mL/kg, 4 h) after tracheotomy and intubation, and the respiratory frequency was 140 times/min. VILI group: mice underwent mechanical ventilation (20 mL/kg, 4 h) after tracheotomy and intubation, and the respiratory frequency was 100 times/min. VILI + Re group: based on the VILI group, mice were intraperitoneally injected with 16 mg/kg Re. (A,B) Macrophage pyroptosis is represented by the caspase-1- and PI-positive cells (flow cytometry assay). (C–J) GSDMD, cleaved GSDMD, HSP90, NLRP3, IL-1β, caspase-1, TSPO, and GAPDH protein levels in macrophages (Western blot). GSDMD and cleaved GSDMD levels were normalized by the HSP90 level. NLRP3, IL-1β, caspase-1, and TSPO levels were normalized by GAPDH level. $^{*}p < 0.05$, $^{**}p < 0.01$, $^{***}p < 0.001$ vs. the Sham group. $^{+++}p < 0.001$ vs. VILI the group. $^{\theta}p < 0.05$, $^{\theta\theta\theta}p < 0.001$ vs. the Re group. All assays were repeated thrice. PI, propidium iodide; GSDMD, gasdermin D; HSP90, heat shock protein 90; NLRP3, NOD-like receptor thermal protein domain associated protein 3; TSPO, translocator protein; GAPDH, glyceraldehyde-3-phosphate dehydrogenase.

up-regulation of caspase-1^{+} cells, the cleaved GSDMD/GSDMD value, NLRP3, IL-1β, and caspase-1 in the VILI group (Fig. 2A–H, $p < 0.001$); the opposite trends were detected in the Re group (Fig. 2A–H, $p < 0.001$). There was an increase in caspase-1^{+} cells in the VL group (Fig. 2A,B, $p < 0.001$). Of note, the VILI-induced up-regulation was confirmed to be reversed by Re based on a comparison of the VILI + RE group with the Re group (Fig. 2A–H, $p < 0.05$). Moreover, our data showed that the caspase-1 protein level was significantly reduced by Re compared to the sham group, and this reduction was offset by VILI in the VILI + RE group (Fig. 2E,H, $p < 0.001$).

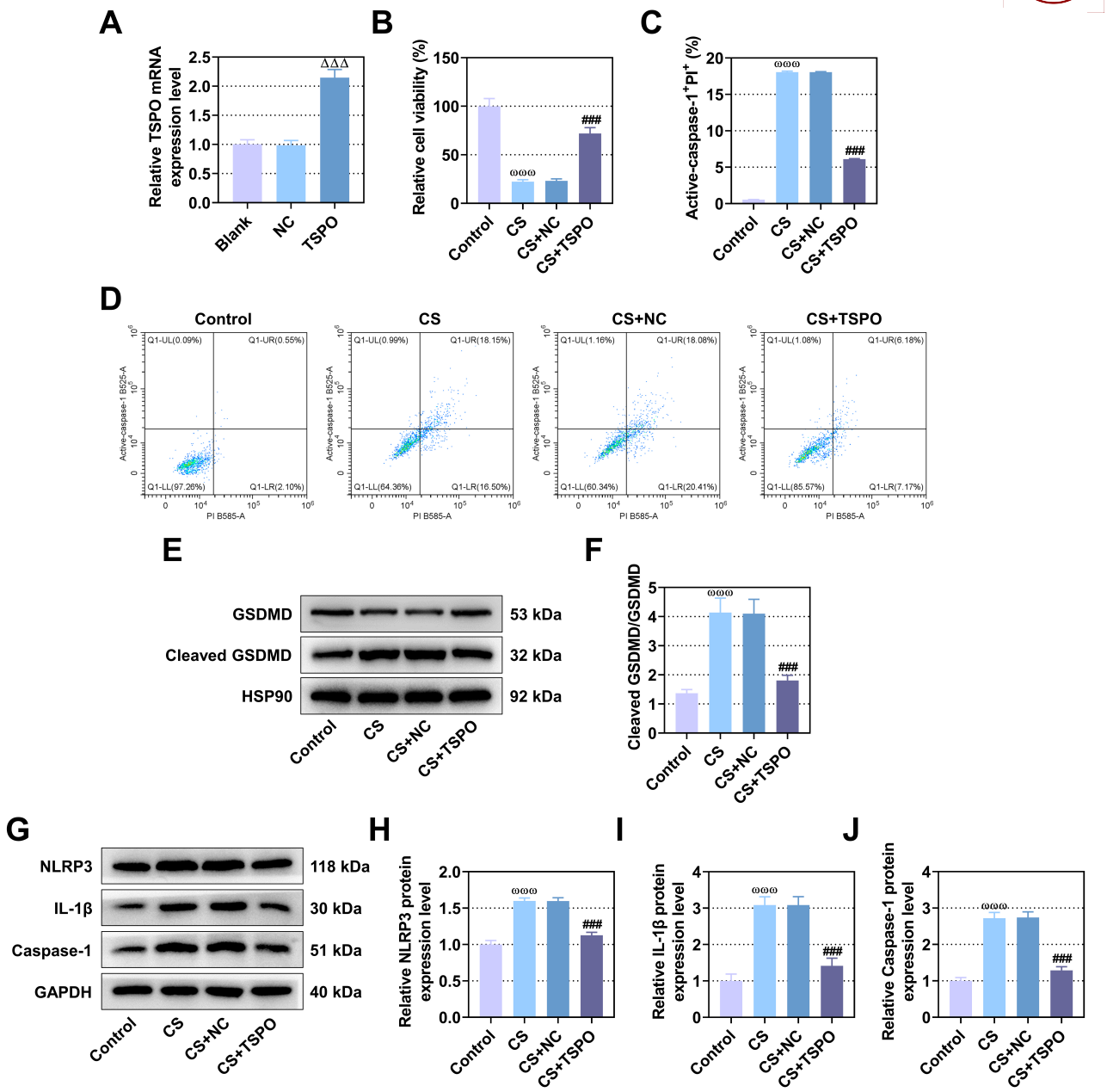

Fig. 3. Re blocked macrophage pyroptosis by activating TSPO. Macrophages were isolated from mouse BALF. For (A), macrophages were transfected with/without pDONR223 vector/TSPO plasmid. (A) TSPO mRNA level in macrophages (qRT-PCR, GAPDH as internal reference). For (B–J), macrophages were distributed into four groups. Control group: macrophages were loaded in the Flexercell FX-4000T strain unit without mechanical stretching. CS group: macrophages received mechanical stretching (4 h). CS + NC or TSPO group: macrophages received mechanical stretching (4 h) and transfected with pDONR223 vector or TSPO plasmid. (B) Macrophage viability (CCK-8 assay). (C,D) Macrophage pyroptosis is represented by the caspase-1- and PI-positive cells (flow cytometry assay). (E–J) GSDMD, cleaved GSDMD, HSP90, NLRP3, IL-1β, caspase-1, and GAPDH protein levels in macrophages (Western blot). GSDMD and cleaved GSDMD levels were normalized by the HSP90 level. NLRP3, IL-1β and caspase-1 levels were normalized by GAPDH level. $^{\Delta\Delta\Delta}p < 0.001$ vs. the NC group. $^{\omega\omega\omega}p < 0.001$ vs. the Control group. $^{\#\#\#}p < 0.001$ vs. the CS + NC group. All assays were repeated three times. CS, cell stretch; NC, negative control; qRT-PCR, quantitative real time polymerase chain reaction; CCK-8, cell counting kit-8.

Re Blocked Macrophage Pyroptosis by Activating TSPO

We found Re significantly increased the TSPO level in macrophages (Fig. 2I,J, $p < 0.01$), whereas the level was significantly reduced in the VILI group (Fig. 2I,J, $p < 0.05$); however, the reduction in the VILI group was counteracted by Re (Fig. 2I,J, $p < 0.001$).

To elucidate whether Re alleviated macrophage pyroptosis by activating TSPO, TSPO was overexpressed in macrophages. qRT-PCR results revealed TSPO was successfully overexpressed in macrophages (Fig. 3A, $p < 0.001$). CS was applied to simulate the mechanical ventilation *in vitro*. Our data revealed that macrophage viability was significantly inhibited in the CS group (Fig. 3B, $p < 0.001$). Macrophage pyroptosis was clearly increased under the treatment of CS, as indicated by the increases in caspase-1$^+$ cells, the cleaved GSDMD/GSDMD value, NLRP3, IL-1β, and caspase-1 (Fig. 3C–J, $p < 0.001$). Of note, these influences of CS on macrophage viability and pyroptosis were reversed by overexpression of TSPO (Fig. 3B–J, $p < 0.001$).

Discussion

Reducing alveolar macrophage pyroptosis is considered a promising therapy for the treatment of VILI [11]. Re can inhibit pyroptosis by suppressing the production of inflammatory factors [15]. In this study, we explored the molecular mechanism of Re mitigation of VILI. Our outcomes clearly showed that Re alleviated VILI by activating TSPO to inhibit macrophage pyroptosis.

Previous studies have shown that the VILI model in rodents plays an indispensable role in exploring the pathomechanism of VILI [18,22]. VILI is accompanied by damaged lung tissues, and increases in the lung W/D weight ratio, lung EBA permeability index, and BALF protein content [18,23,24]; these changes were also found in our VILI model mice. Re has been reported to improve bronchopneumonia-induced lung injury and reduce the lung W/D weight ratio [10], suggesting that Re could also play a role in VILI. Our results indicated that Re can alleviate VILI, as confirmed by the reductions in the lung injury score, W/D weight ratio, EBA permeability index, and BALF protein content. These results support the potential application of Re in treating VILI.

Reportedly, the inflammatory response is closely associated with the pathogenesis of VILI [25]. Consistent with earlier findings [18], our data revealed that the inflammation-related factors (MPO, MDA, 8-OHdG, IL-6, TNF-α, MIP-2, IL-1β, and IL-18) were significantly increased in VILI. The previous study has shown that Re can alleviate bronchopneumonia by suppressing the inflammatory response [10]. Here, we demonstrated that Re improved the inflammatory response during VILI by downregulating these inflammatory factors, indicating the anti-inflammatory effect of Re in VILI.

Furthermore, in VILI, alveolar macrophages are activated to generate pro-inflammatory factors, together with macrophage pyroptosis [11]; these effects were also confirmed in our research. As a newly described mode of programmed cell death, pyroptosis is usually induced by certain inflammasomes [26,27]. Among them, the NLRP3 inflammasome is a kind of multimeric cytoplasmic protein complex, which is aggregated in response to cell disturbance. The aggregation of the NLRP3 inflammasome contributes to the activation of caspase-1, cleaving of GSDMD, and release of inflammatory factors (such as IL-1β and IL-18), which then results in inflammatory cell death (pyroptosis) [28–31]. Intriguingly, the inhibition of pyroptosis can alleviate VILI [12], and Re can dampen pyroptosis by downregulating the NLRP3 inflammasome and the release of inflammatory factors [10,15]. In this study, we revealed that Re suppressed macrophage pyroptosis induced by VILI, suggesting that Re can alleviate VILI by inhibiting macrophage pyroptosis.

In addition, we confirmed that Re promoted TSPO expression in alveolar macrophages. Reportedly, TSPO is involved in the progression of VILI [32]. Yet, in different physiological conditions, the function of TSPO *in vivo* is still disputed [33]. After silencing of TSPO, macrophage pyroptosis is accelerated [17], indicating the potential effect of TSPO on mitigating macrophage pyroptosis. Our data demonstrated that TSPO overexpression suppressed the CS-induced macrophage pyroptosis *in vitro*. Combined with the above reports, these results indicate that Re may alleviate VILI by promoting TSPO to inhibit macrophage pyroptosis. However, the mechanism by which Re impacts macrophage pyroptosis has not been fully elucidated here, which is one of the limitations of our study, and this topic will be further investigated in the future. In future studies, animal experiments also will be designed to test our findings.

Conclusion

In summary, our results reveal an underlying mechanism for the effect of Re on VILI, and verify the inhibitory effect of Re on macrophage pyroptosis during VILI. Mechanistically, we confirm that Re alleviates VILI by activating TSPO to dampen macrophage pyroptosis, indicating that TSPO may serve as a critical target to improve VILI.

Availability of Data and Materials

The analyzed data sets generated during the study are available from the corresponding author upon reasonable request.

Author Contributions

LZ designed the research study; DZ and HL performed the research; XJ collected and analyzed the data. All authors have been involved in drafting the manuscript and all authors have been involved in revising it critically for important intellectual content. All authors have given the final approval of the version to be published. All authors have participated sufficiently in the work to take public responsibility for appropriate portions of the content and agreed to be accountable for all aspects of the work in ensuring that questions related to its accuracy or integrity.

Ethics Approval and Consent to Participate

The experimental operations on C57BL/6 mice were approved by the Ethics Committee of the Affiliated Jinhua Hospital, Zhejiang University School of Medicine for Experimental Animals Welfare (No. AL-JHYY202353).

Acknowledgment

Not applicable.

Funding

This work was supported by the Key Project for Science and Technology Bureau of Jinhua Municipal (2023-3-120) and the Applied Research Project of Public Welfare for Science and Technology Department of Zhejiang Province (LGF19H010008).

Conflict of Interest

The authors declare no conflict of interest.

Supplementary Material

Supplementary material associated with this article can be found, in the online version, at https://doi.org/10.24976/Discov.Med.202436187.146.

References

[1] Paudel R, Trinkle CA, Waters CM, Robinson LE, Cassity E, Sturgill JL, *et al*. Mechanical Power: A New Concept in Mechanical Ventilation. The American Journal of the Medical Sciences. 2021; 362: 537–545.

[2] Tsumura H, Harris E, Brandon D, Pan W, Vacchiano C. Review of the Mechanisms of Ventilator Induced Lung Injury and the Principles of Intraoperative Lung Protective Ventilation. AANA Journal. 2021; 89: 227–233.

[3] Ye L, Zeng Q, Ling M, Ma R, Chen H, Lin F, *et al*. Inhibition of IP3R/Ca2+ Dysregulation Protects Mice From Ventilator-Induced Lung Injury *via* Endoplasmic Reticulum and Mitochondrial Pathways. Frontiers in Immunology. 2021; 12: 729094.

[4] Wang Y, Xie W, Feng Y, Xu Z, He Y, Xiong Y, *et al*. Epithelial-derived exosomes promote M2 macrophage polarization via Notch2/SOCS1 during mechanical ventilation. International Journal of Molecular Medicine. 2022; 50: 96.

[5] Huang H, Feng H, Zhuge D. M1 Macrophage Activated by Notch Signal Pathway Contributed to Ventilator-Induced Lung Injury in Chronic Obstructive Pulmonary Disease Model. The Journal of Surgical Research. 2019; 244: 358–367.

[6] Yin D, Wang W, Han W, Fan C. Targeting Notch-activated M1 macrophages attenuate lung tissue damage in a rat model of ventilator induced lung injury. International Journal of Molecular Medicine. 2019; 44: 1388–1398.

[7] Liu X, Lin S, Zhong Y, Shen J, Zhang X, Luo S, *et al*. Remimazolam Protects Against LPS-Induced Endotoxicity Improving Survival of Endotoxemia Mice. Frontiers in Pharmacology. 2021; 12: 739603.

[8] Keam SJ. Remimazolam: First Approval. Drugs. 2020; 80: 625–633.

[9] Lim BG, Lee IO. Anesthetic management of geriatric patients. Korean Journal of Anesthesiology. 2020; 73: 8–29.

[10] Yang M, Li L. Remimazolam attenuates inflammation in bronchopneumonia through the inhibition of NLRP3 activity by PDPK1 ubiquitination. Chemical Biology & Drug Design. 2024; 103: e14438.

[11] Dai M, Li Q, Pan P. The Modulation of Interferon Regulatory Factor-1 via Caspase-1-Mediated Alveolar Macrophage Pyroptosis in Ventilator-Induced Lung Injury. Mediators of Inflammation. 2022; 2022: 1002582.

[12] Ling M, Ye L, Zeng Q, Li Z, He S, Lin J, *et al*. Ferrostatin-1 alleviates ventilator-induced lung injury by inhibiting ferroptosis. International Immunopharmacology. 2023; 120: 110356.

[13] Hu J, Cheng M, Jiang C, Liu L, He Z, Liu L, *et al*. Deferoxamine Mitigates Ferroptosis and Inflammation in Hippocampal Neurons After Subarachnoid Hemorrhage by Activating the Nrf2/TXNRD1 Axis. Molecular Neurobiology. 2024; 61: 1044–1060.

[14] Huang Y, Xu W, Zhou R. NLRP3 inflammasome activation and cell death. Cellular & Molecular Immunology. 2021; 18: 2114–2127.

[15] Shi M, Chen J, Liu T, Dai W, Zhou Z, Chen L, *et al*. Protective Effects of Remimazolam on Cerebral Ischemia/Reperfusion Injury in Rats by Inhibiting of NLRP3 Inflammasome-Dependent Pyroptosis. Drug Design, Development and Therapy. 2022; 16: 413–423.

[16] Nutma E, Ceyzériat K, Amor S, Tsartsalis S, Millet P, Owen DR, *et al*. Cellular sources of TSPO expression in healthy and diseased brain. European Journal of Nuclear Medicine and Molecular Imaging. 2021; 49: 146–163.

[17] Zhang X, Han J, Xu Y, Cai M, Gao F, Han J, *et al*. TSPO Deficiency Exacerbates GSDMD-Mediated Macrophage Pyroptosis in Inflammatory Bowel Disease. Cells. 2022; 11: 856.

[18] Ruan H, Li W, Wang J, Chen G, Xia B, Wang Z, *et al*. Propofol alleviates ventilator-induced lung injury through regulating the Nrf2/NLRP3 signaling pathway. Experimental and Molecular Pathology. 2020; 114: 104427.

[19] Chen S, Bai Y, Xia J, Zhang Y, Zhan Q. Rutin alleviates ventilator-induced lung injury by inhibiting NLRP3 inflammasome activation. iScience. 2023; 26: 107866.

[20] Liu Y, Tang G, Li J. Long non-coding RNA NEAT1 participates in ventilator-induced lung injury by regulating miR-20b expression. Molecular Medicine Reports. 2022; 25: 66.

[21] Luo Y, Tang H, Zhang Z, Zhao R, Wang C, Hou W, *et al*. Pharmacological inhibition of epidermal growth factor receptor attenuates intracranial aneurysm formation by modulating the phenotype of vascular smooth muscle cells. CNS Neuroscience & Therapeutics. 2022; 28: 64–76.

[22] Joelsson JP, Ingthorsson S, Kricker J, Gudjonsson T, Karason S. Ventilator-induced lung-injury in mouse models: Is there a trap? Laboratory Animal Research. 2021; 37: 30.

[23] Ju YN, Geng YJ, Wang XT, Gong J, Zhu J, Gao W. Endothelial Progenitor Cells Attenuate Ventilator-Induced Lung Injury with Large-Volume Ventilation. Cell Transplantation. 2019; 28: 1674–1685.

[24] Wang W, Yang Y, Wang L, Guo X, Tian L, Wang H, *et al*. Sevoflurane alleviates ventilator-induced lung injury in rats by down-regulating the TRPV4/C-PLA2 signaling pathway. Nan Fang Yi Ke Da Xue Xue Bao. 2023; 43: 1886–1891. (In Chinese)

[25] Vishnupriya S, Priya Dharshini LC, Sakthivel KM, Rasmi RR. Autophagy markers as mediators of lung injury-implication for therapeutic intervention. Life Sciences. 2020; 260: 118308.

[26] Bai B, Yang Y, Wang Q, Li M, Tian C, Liu Y, *et al*. NLRP3 inflammasome in endothelial dysfunction. Cell Death & Disease. 2020; 11: 776.

[27] Jin H, Xie W, He M, Li H, Xiao W, Li Y. Pyroptosis and

Sarcopenia: Frontier Perspective of Disease Mechanism. Cells. 2022; 11: 1078.

[28] Fang Y, Tian S, Pan Y, Li W, Wang Q, Tang Y, *et al*. Pyroptosis: A new frontier in cancer. Biomedicine & Pharmacotherapy. 2020; 121: 109595.

[29] Li S, Sun Y, Song M, Song Y, Fang Y, Zhang Q, *et al*. NLRP3/caspase-1/GSDMD-mediated pyroptosis exerts a crucial role in astrocyte pathological injury in mouse model of depression. JCI Insight. 2021; 6: e146852.

[30] Yan H, Luo B, Wu X, Guan F, Yu X, Zhao L, *et al*. Cisplatin Induces Pyroptosis via Activation of MEG3/NLRP3/caspase-1/GSDMD Pathway in Triple-Negative Breast Cancer. International Journal of Biological Sciences. 2021; 17: 2606–2621.

[31] Ding P, Yang R, Li C, Fu HL, Ren GL, Wang P, *et al*. Fibroblast growth factor 21 attenuates ventilator-induced lung injury by inhibiting the NLRP3/caspase-1/GSDMD pyroptotic pathway. Critical Care (London, England). 2023; 27: 196.

[32] Deniel G, Dhelft F, Lancelot S, Orkisz M, Roux E, Mouton W, *et al*. Pulmonary inflammation decreases with ultra-protective ventilation in experimental ARDS under VV-ECMO: a positron emission tomography study. Frontiers in Medicine. 2024; 11: 1338602.

[33] Wang H, Zhai K, Xue Y, Yang J, Yang Q, Fu Y, *et al*. Global Deletion of TSPO Does Not Affect the Viability and Gene Expression Profile. PLoS ONE. 2016; 11: e0167307.